A pFFT Accelerated Linear Strength BEM Potential Solver

D.J. Willis, J.K. White and J. Peraire
Massachusetts Institute of Technology,
Room 36-866, 77 Massachusetts Ave., Cambridge, MA 02139, USA
{djwillis, white, peraire }@mit.edu

ABSTRACT

A linear strength, Galerkin Boundary Element Method (BEM) for the solution of the three dimensional, direct potential boundary integral equation is presented. The method incorporates node based linear shape functions of the single and double layers on flat triangular elements. The BEM solution is accelerated using a precorrected Fast Fourier Transform algorithm (pFFT) [1]. Due to the extended compact support of the linear basis, there exist several approaches for implementing a linear strength pFFT. In this paper, two approaches are discussed and results are presented for the simpler of the two implementations.

The work presented in this paper is applied to potential flow problems. Results are presented for flow solutions around spheres and aircraft wings. The results of the sphere simulations are compared with analytical solutions, while the solutions for the wings are compared with 2-Dimensional results. The results indicate accurate solutions of the potential flow around 3-Dimensional bodies. The linear basis shows improved accuracy when compared with the constant basis approach; however, the error of the linear BEM solution converges at a similar rate to the constant panels. This is due to the domination of the surface discretization error, which converges in the first order for planar element representations of curved surfaces.

Keywords: pfft, linear, potential, BEM, Galerkin

1 Introduction

The rapid and accurate solution of Laplace's equation for arbitrary exterior 3-Dimensional domains is beneficial in many diverse applications. With centuries of theoretical analysis and decades of computational work, there is still considerable interest in solving Laplace's equation faster and more accurately.

In order to augment the solution accuracy, a linear order basis function was explored in this work. Several implementations of higher order boundary element methods have been presented in the past[2][3]. More recently there have been many other high order BEM implementations, however, the majority of current implementations of the BEM are still constant collocation approaches. This is due to the simplicity of the constant collocation method as well as the solution accuracy vs. time tradeoff.

The precorrected Fast Fourier Transform(pFFT) is used to minimize the solution time for the current linear BEM solver. The pFFT uses a regular grid to approximately account for the farfield interactions. Grid based computations of the farfield interactions derive their ancestry from research dating back to Hockney and Eastwood [4]. Phillips and White [1] originally proposed the pFFT approach for potential solutions in electrostatics, however its use is now widespread [5][6][7]. The pFFT algorithm enables solution times proportional to $nlog(n)$ where n is the number of unknowns.

In section 2 a brief description of the governing boundary integral equation for potential flow is presented, followed by an introduction to the linear basis Galerkin approach used in this implementation. In section 3, two possible linear pFFT implementations are described. Results and conclusions for the simpler of the two pFFT implementations are presented in sections 4 and 5 respectively.

2 The Boundary Integral Equation Formulation For Potential Flow

The potential flow equation approximates flows with large Reynolds Numbers, $Re \sim O(10^6 \rightarrow \infty)$, where Re is a non-dimensional measure of inertia forces to viscous forces. Potential flows are ones in which the fluid can be approximated as inviscid, incompressible, steady and irrotational. The direct boundary integral equation form of the potential flow equation is used in this work:

$$\phi(\vec{x}) = \frac{1}{4\pi}\int_S \frac{\partial \phi}{\partial n} G(\vec{x},\vec{x}')dS'_B - \frac{1}{4\pi}\int_S \phi \frac{\partial}{\partial n} G(\vec{x},\vec{x}')dS'_B,$$

where the Green's function, is $G(\vec{x},\vec{x}') = \frac{1}{\|\vec{x}-\vec{x}'\|}$. The perturbation velocity denoted as ϕ, is such that $\nabla\phi = \vec{v}$, where $\vec{v}$ is the velocity of the perturbed fluid in the domain. $\vec{x}$ is the position of the evaluation point, $\vec{x}'$ is a variable representing the position on the body, S'_B is the body surface area, and n is the normal vector of the body surface at $\vec{x}'$.

For any surface of a solid body we expect a no pen-

etration, zero flux body boundary condition:

$$\nabla\phi(\vec{x}_b)\cdot\hat{n}(\vec{x}_b) = -\vec{V}_\infty\cdot\hat{n}(\vec{x}_b) \rightarrow \frac{\partial\phi}{\partial n} = -\vec{V}_\infty\cdot\vec{n}.$$

In limit as $\vec{x}$ tends to infinity, the farfield velocity tends toward zero, or:

$$\lim_{\vec{x}\rightarrow\infty}\nabla\phi(\vec{x}) \rightarrow \frac{1}{|\vec{x}|^3}.$$

The pressure at any point in the fluid is related to the velocity using Bernoulli's equation, which is a simplified version of the Navier Stokes equations corresponding to the potential flow approximations:

$$\rho\frac{\|\vec{v}+\vec{V}_\infty\|\cdot\|\vec{v}+\vec{V}_\infty\|}{2} + p = Constant = P_\infty,$$

where ρ is the fluid density, p is the static pressure, and P_∞ is the stagnation pressure in the fluid domain.

2.1 Linear Varying Element Strength

The linear strength BEM is implemented using a node based, triangular element discretization of the surface, with a Galerkin formulation to force the boundary conditions on the surface. The result is an equation for each target basis i on the surface:

$$4\pi\cdot\int_{S_{T_i}}\psi_i\cdot\phi(\vec{x})dS_{T_i} =$$

$$\sum_{j=1}^{N_b}\int_{S_{T_i}}\psi_i\cdot\int_{S'_{B_j}}(-\vec{V}_\infty\cdot n)G(\vec{x},\vec{x}')dS'_{B_j}dS_{T_i}$$

$$-\sum_{j=1}^{N_b}\int_{S_{T_i}}\psi_i\cdot\int_{S_{B_j}}\phi\frac{\partial}{\partial n}\left(G(\vec{x},\vec{x}')\right)dS'_{B_j}dS_{T_i},$$

where ψ_i is the target linear Galerkin tent basis, S_{T_i} is the target basis function area, and S_{B_j} is the j-th linear source basis function, $j\in\{1,...,N_b\}$, and N_b is the number of basis functions. In the integrals above, the distributions of ϕ and $\frac{\partial\phi}{\partial n}$ are approximated using node based, linear tent basis functions.

Due to the complexity of the above integration over the source and target panels, only the inner integral or the outer integral can be computed analytically. In this work, the inner integral is computed using analytic closed form expressions based on [8] while the outer integral is computed using Gauss Quadrature. If care is taken, computing the integrals for all three linear shape functions is slightly more expensive than a single constant strength panel computation. There is however, an increase in computation time due to the use of a Galerkin approach. The Galerkin integral is computed using Gaussian Quadrature which requires a panel integral evaluation for each of the quadrature points on the target basis.

The boundary integral equation, when applied to a discretized surface, becomes a linear algebraic equation for the potential on the surface of the body as follows:

$$[A_{n\times n}]\,\vec{\phi} = [B_{n\times n}]\cdot(-\vec{V}\cdot\hat{n}) \qquad (1)$$

The resulting influence matrices, $A_{n\times n}$ (double layer influence) and $B_{n\times n}$ (single layer influence) are fully dense. The $n\times n$ corresponds to the interaction of the n basis functions in the system. The cost of fully computing all of the elements in the direct matrices is $O(n^2)$, while the cost of a full direct linear system solution is $O(n^3)$. The costs set practical limits on discretization fineness. To reduce complexity, the pFFT is considered to accelerate the system solution.

3 pFFT Acceleration

In this work we implemented a pFFT[1] approach (via a modification of the pFFT++[7] code) to approximately calculate the matrix vector products (MVP) in a GMRES [9] iterative solution technique for solving (1). The pFFT algorithm is summarized in the following steps (more detail is available in [1],[7]):
1) The surface strengths (panel charges) are projected onto a uniform FFT grid.
2) The convolution to determine the potential at the grid points is computed as a multiplication after an FFT.
3) The resulting grid values (potential) are projected back onto the surface of the discretized body.
4) The solution is corrected to account for the near-field panel interactions exactly via direct integration.

The following equation represents a matrix equation of the pFFT solution process:

$$[A]\,\vec{\phi} = \left[IHP + \left[\tilde{D} - \tilde{I}\tilde{H}\tilde{P}\right]_{Local}\right]\vec{\phi}$$

Where, A, is the influence matrix acting on $\vec{\phi}$, I, is the interpolation matrix, H, is the FFT matrix, P, is the projection matrix. The term $\left[\tilde{D} - \tilde{I}\tilde{H}\tilde{P}\right]_{Local}$ is the local direct correction, or appropriately named, the precorrection.

The implementation of the pFFT for linear strength basis functions is presented below. The first approach is a panel-to-panel interaction. This is implemented in the current linear pFFT algorithm. The second approach is a full tent-basis-function-to-tent-basis-function approach. The second approach is more memory efficient, and potentially more time efficient than the panel-to-panel based approach. The implementation of the second approach has not been attempted to date.

3.1 Panel based linear shape function pFFT

In the panel-to-panel approach, each linear tent basis is deconstructed into individual panels, each with

three linear shape functions. A pFFT is constructed using each of the three shape functions on a panel. Once the panel based pFFT components are constructed, the MVP can be computed by deconstructing the vector in the MVP from a tent basis into a panel basis. Following the deconstruction, the MVP is computed as a panel to panel interaction via the individual panel based shape functions. Once the MVP is complete for the panel to panel interactions the linear tent basis representation of the solution is constructed. A benefit of using this approach, is the machinery of the constant collocation pFFT is easily modified. As a result, a general method incorporating both linear and constant panels can be implemented with ease. The panel based linear pFFT is represented in matrix form as:

$$[A]\,\vec{\phi} = J^T \left[I_P H P_P + \left[\tilde{D_P} - \tilde{I_P} \tilde{H} \tilde{P_P} \right]_{Local} \right] J\vec{\phi}$$

Where, J is the operator used to decompose the tent basis into a panel based representation. J^T is the operator to reconstruct the tent basis from the individual panels. The subscript P represents a panel-to-panel interaction.

The main differences between the panel-to-panel approach and the constant collocation approach lie in:
a) The projection and interpolation involve three linear shape functions per panel rather than one, as seen in the constant case.
b) The direct interaction computation is a 3×3 interaction of the linear shape functions, rather than a single panel-to-collocation-point interaction.

3.2 Tent based linear shape function pFFT

A more memory optimal high order pFFT algorithm can be obtained by considering each complete tent function as an element basis. This causes the extended support to play a more significant role in the projection, interpolation and direct computations. As a result of considering full node based basis functions, the memory usage will be lower than the method proposed in section 3.1, however, care must be taken during the construction of the direct matrix in order to minimize the number of panel integral computations.

4 Results

In figure 1, we present the solution of the potential flow around a unit sphere. The potential, according to the analytical solution, varies linearly in the flow direction, from $\phi = +0.5$ at the leading edge point, to $\phi = -0.5$ at the trailing edge point. As can be seen in figure 1, solution by the linear BEM implementation compares well with the analytic solution. In figure 2 the convergence of the error in the potential over the surface

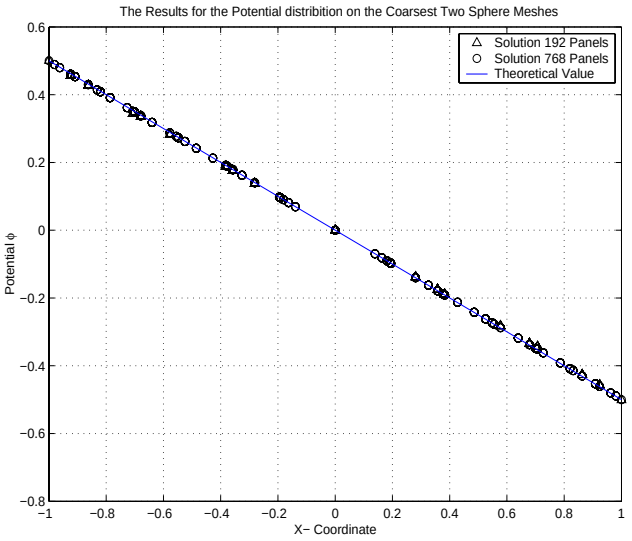

Figure 1: The solution of the potential flow around a 192 panel and 768 panel sphere compared with the analytical solution. Notice there is very good agreement between the analytical solution and the computed solution even with a relatively coarse distribution.

with increasing number of panels in the discretization is shown. The error is computed in the L2-norm for the linear and constant Galerkin formulations. Figure

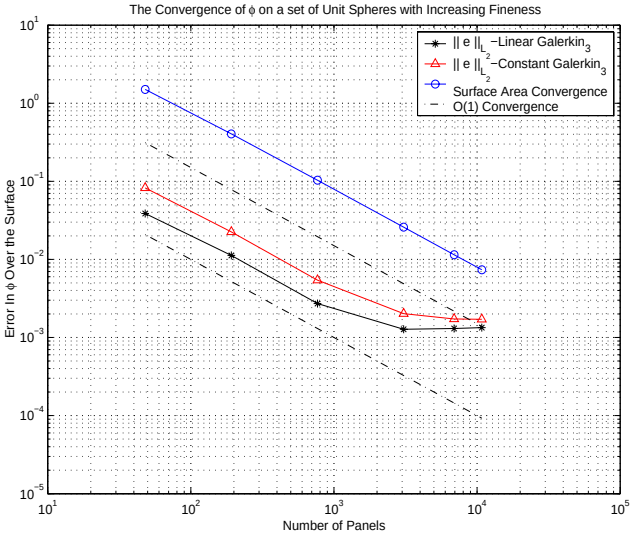

Figure 2: The error in Potential over the surface measured in an L_2-norm for both the constant and linear Galerkin BEM, for increasingly refined surface meshes over the unit sphere. In addition, the convergence of the surface area is shown.

2 shows that the linear basis BEM approach is consistently more accurate than the constant case; however, the convergence rate of the linear strength cases is sim-

ilar to that of the constant strength cases. The trend in convergence, is due to the dominance of the discretization error in the computation. In order to confirm this result, further investigation of the convergence rate can be performed through the use of a curved panel discretization. The convergence rate of the error shown in figure 2 reaches a point where the error stays nearly constant with increased fineness of discretization. This is due to the accuracy of the pFFT farfield approximation.

In figure 3, a complex geometry is presented for which an analytic solution is not known. The pressure coefficient is shown for a finite 3-Dimensional rectangular aircraft wing with a NACA 0012 airfoil and a high aspect ratio. In the limit of infinite aspect ratio, the pressure distribution at the centerline of the wing mimics two dimensional flow. The results presented in figure 3 show that there is a good agreement with 2-Dimensional results[10].

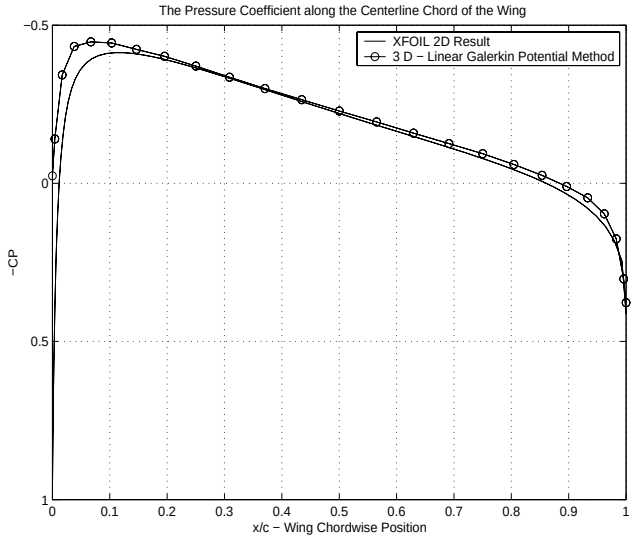

Figure 3: The plot of the surface pressure coefficient at the centerline of a NACA 0012 large aspect ratio wing, compared with a 2-Dimensional airfoil solution from XFOIL [10]

5 Conclusions

A linear strength implementation of a pFFT accelerated BEM for the solution of potential problems which scales with $O(nlog(n))$ (n is the number of panels) has been presented. Two approaches for computing a pFFT accelerated MVP are described, one simple, and the other more complex and optimal from a memory standpoint. Furthermore, we have shown results for the panel-to-panel implementation of the linear pFFT. In sphere test cases, the convergence rate of the linear pFFT was not increased compared with the constant BEM, however, the linear strength panels do show increased solution accuracy. The planar panel representation of the surface dominates the convergence of the solution. Should an increased convergence rate be desired, one should investigate eliminating the discretization error through the use of curved panels.

6 Acknowledgments

The authors would like to thank the Singapore-MIT Alliance and the National Science Foundation for their generous support of this work.

REFERENCES

[1] J. R. Phillips, J.K. White, "A Precorrected-FFT Method for Electrostatic Analysis of Complicated 3-D Structures," IEEE Transactions On Computer-Aided Design of Integrated Circuits and Systems, IEEE, Vol. 16, 1997.

[2] J.L. Hess, D.M. Friedman, "An Improved High-Order Panel Method for Three-Dimensional Lifting Flow," Douglas Aircraft Co., Rep. No. NADC-79277-60, 1981.

[3] R.L. Carmichael,L.L. Ericson, "PAN AIR – A High Order Panel Method For Predicting Subsonic of Supersonic Linear Potential Flows About Arbitrary Configurations," AIAA Paper 81-1255, June 1981.

[4] R. Hockney, J. Eastwood, "Computer Simulation Using Particles", McGraw-Hill, New York. 1981.

[5] S. Kuo, M. Altman, J. Bardhan, B. Tidor and J. White, "Fast Methods for Simulation of Biomolecule Electrostatics," Proc. of IEEE Conference on Computer-Aided Design, San Jose, November 2002.

[6] N.R. Aluru, V. Nadkarni, and J. White,"A parallel Precorrected-FFT Based Capacitance Extraction Program for Signal Integrity Analysis," Proceedings of the 33rd Design Automation Conference, Las Vegas, June, 1996.

[7] Zhenhai Zhu, Song, B., White J. "Algorithms in fastimp: a fast and wideband impedance extraction program for complicated 3-D geometries," Design Automation Conference, 2003.

[8] J.N. Newman, "Distribution of Sources and Normal Dipoles Over a Quadrilateral Panel,"Journal of Engineering Mathematics, Vol. 20, 1985.

[9] Y. Saad, M. Schultz, "GMRES: A Generalized Minimal Residual Algorithm for Solving Non symmetric Linear Systems," SIAM, Journal of Sci. Stat. Comput., Vol. 7, 1986.

[10] M. Drela, "XFOIL: An Analysis and Design System for Low Reynolds Number Airfoils," Conference on Low Reynolds Number Airfoil Aerodynamics, 1989.